MDPI

Article

Quantitative Determination of Diosmin in Tablets by Infrared and Raman Spectroscopy

Sonia Pielorz [ID], Magdalena Węglińska, Sylwester Mazurek [ID] and Roman Szostak *[ID]

Department of Chemistry, University of Wrocław, 14 F. Joliot-Curie, 50-383 Wrocław, Poland
* Correspondence: roman.szostak@chem.uni.wroc.pl; Tel.: +48-71-3757-307

Abstract: Diosmin is widely used in the treatment of chronic venous diseases and hemorrhoids. Based on Raman and infrared reflection spectra of powdered tablets in the mid- and near-infrared regions and results of reference high-performance liquid chromatographic analysis, partial least squares models that enable fast and reliable quantification of the studied active ingredient in tablets, without the need for extraction, were elaborated. Eight commercial preparations containing diosmin in the 66–92% (w/w) range were analyzed. In order to assess and compare the quality of the developed chemometric models, the relative standard errors of prediction for calibration and validation sets were calculated. We found these errors to be in the 1.0–2.4% range for the three spectroscopic techniques used. Diosmin content in the analyzed preparations was obtained with recoveries in the 99.5–100.5% range.

Keywords: diosmin; Raman; infrared; NIR; quantitative analysis; pharmaceutical preparations; PCA; PLS

1. Introduction

Diosmin, a 7-rhamnoglucoside of 3′,5,7-trihydroxy-4′-methoxyflavone, IUPAC name of 5-hydroxy-2-(3-hydroxy-4-methoxyphenyl)-7-[(2S,3R,4S,5S,6R)-3,4,5-trihydroxy- 6-[[(2R,3R, 4R,5R,6S)-3,4,5-trihydroxy-6-methyloxan-2-yl]oxymethyl]oxan-2-yl]oxychro-en-4-one, is a chemical compound belonging to a group of flavonoids originating in the Rutaceae family [1]. It was first isolated in 1925 from Scrophularia nodosa L. [2]. Diosmin is a gray-yellow powder. Similar to other flavonoids, it dissolves poorly in polar and nonpolar protic solvents but much better in aprotic solvents (e.g., DMSO) [3]. The poor solubility of diosmin in most solvents creates a problem when it is used as a drug. For this reason, various technological processes are applied, including micronization, to increase the solubility and thus bioavailability of this flavonoid [4]. Currently, diosmin is isolated from the flesh, skin and seeds of citrus fruits (Citrus genus), mainly from the fruits of bitter orange (Citrus aurantium). It is obtained synthetically from hesperidin through treatment with an aqueous solution of sodium hydroxide in the presence of iodine and pyridine with an efficiency of 66% or in the process of acetyl hesperidin bromination using N-bromosuccinimide, benzoyl peroxide and chloroform, achieving an efficiency equal to 44%, as well as using ionic liquids [5,6]. The obtained compound may be accompanied by various impurities. Their presence affects the quality of the final products. Depending on the method used to process plant material and the synthetic route, diosmin may be contaminated by diosmetin, rhamnose, glucose, eriocitrin and other compounds [7,8]. It is worth noting that diosmin is usually accompanied by hesperidin, from which it is synthesized.

Diosmin is widely used in the treatment of chronic venous insufficiency, hemorrhoids, lymphoedema and varicose veins [9]. Preparations containing diosmin prevent inflammation [10,11] and intensify lymphatic drainage supporting microcirculation [12,13]. These actions reduce symptoms such as swelling, heaviness, cramps and pain in the calves, accelerate the healing of venous ulcers and improve quality of life [14,15]. Diosmin also demonstrates antioxidant [16], antiproliferative [17] and antidiabetic [18] properties. Hundreds

of pharmaceutical preparations containing from 300 to 1000 mg of this active substance in one tablet are distributed all over the world. Therefore, the existing analytical methods are constantly being improved, and new methods are sought for the analysis of this active compound. Several methods can be applied for the determination of diosmin in pharmaceutical preparations. The most frequently used is high-performance liquid chromatography [1]. Among other techniques, thin-layer chromatography [19], voltammetry [20,21] and different spectroscopic methods can be listed [3,22,23]. Prior to analysis, using the enumerated methods, diosmin has to be extracted from the analyzed drug. Extraction is not required when vibrational spectroscopy is applied. Fourier transform infrared and Raman spectroscopy, assisted by multidimensional data analysis techniques, become more and more widely used in the pharmaceutical industry, both for qualitative and quantitative analysis of interesting compounds. These methods are easy to perform and time-efficient compared to chromatographic methods. They enable the analysis of active substances present in pharmaceuticals without active substance extraction or additional sample pre-treatment, which significantly shortens and simplifies the analysis [24–26].

Although the application of near-infrared spectroscopy (NIR) is well established in many areas [27–29], other, less common techniques, including attenuated total reflection (ATR) and diffuse reflectance infrared Fourier transform spectroscopy (DRIFTS) in the mid-infrared region (MIR) and Raman spectroscopy, offer unique possibilities with regard to medicines, foods, body fluids and plant and animal tissue analysis [25,26,29–33]. The most important advantages of these methods include minimal requirements for sample preparation, simplicity of implementation, short analysis time and the ability to automate the process. In combination with chemometrics, they enable fast and detailed qualitative and quantitative analysis of a variety of objects, often in their native form [33–35].

The stable crystal form of diosmin is its monohydrate (Figure 1). The anhydrous form can be prepared by heating DSNM at 110–140 °C. The obtained form is hygroscopic and transforms on air into a monohydrate within 72 h [36]. As a result, diosmin monohydrate is an active pharmaceutical ingredient (API) in commercial preparations.
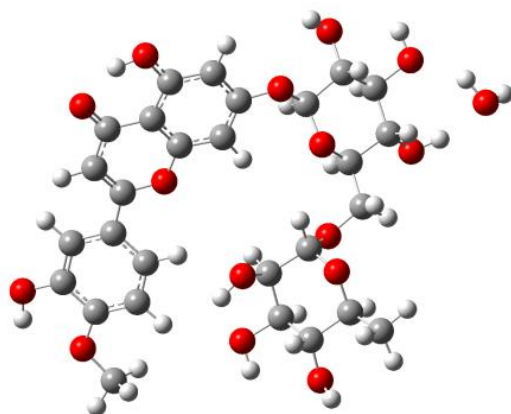
Figure 1. Structure of diosmin hydrate (DSNM).

2. Experiment

2.1. Materials and Sample Preparation

Diosmin was isolated from Preparation 1 (Table S1 in Supplementary Materials). According to manufacturer's declaration, except for diosmin consisting of more than 89% of the tablet weight, magnesium stearate, polyvinyl alcohol and sodium croscarmellose were present. After weighing, tablets were thoroughly pulverized using an FW100 grinder (ChemLand, Stargard, Poland). Next, 14 mL of 0.5 M sodium hydroxide solution was added per tablet. Then, the mixture was vigorously stirred for 15 min, and it was allowed to sit until the next day. The solution was gravity filtered. Next, twice as much demineralized water was added. After 15 min of stirring, 1.2 M hydrochloric acid was added to the solution, to a pH value of 7, to precipitate the diosmin. The pH of the solution was

controlled with universal papers. The mixture was filtered through a Buchner funnel. The resulting precipitate was washed with demineralized water and dried in a desiccator at room temperature. Its purity was checked using the HPLC method. The diosmin was isolated in two series with an efficiency reaching 90%. Raman, MIR and NIR spectra of isolated diosmin were identical with the respective spectra of the diosmin analytical standard (Sigma-Aldrich, Saint Louis, USA). A set of 83 calibration samples, consisting of diosmin, magnesium stearate (Sigma-Aldrich, Saint Louis, MO, USA), polyvinyl alcohol (POCH, Gliwice, Poland) and croscarmellose sodium (Sigma-Aldrich, Saint Louis, MO, USA) (Table S2 in Supplementary Materials) was prepared. Raman, MIR and NIR spectra of diosmin and the remaining ingredients are shown in Figure S1 in Supplementary Materials.

2.2. Reference Analysis

The content of the diosmin and hesperidin was determined (Table S3 in Supplementary Materials) in the analyzed pharmaceutical preparations using high-performance liquid chromatography with diode-array detection (HPLC-DAD). The appropriate amount of powdered tablet, for which the content of diosmin was about 450 mg, was dissolved in 50 mL of a 0.5 M NaOH solution, in a 250 mL volumetric flask. Then, the solution was sonicated for 15 min. After the sample reached room temperature, the volumetric flask was refilled with a mixture of 0.01 M trisodium buffer (pH = 12.4) and methanol (60:40, *v/v*). A total of 25 mL of the prepared solution was diluted again to 100 mL with the aforementioned solvent mixture. The determination of diosmin and hesperidin concentration was carried out in the analyzed preparations with the X-Bridge RP C18 3.5 μm column, 150 × 4.6 mm. The injection volume of the sample was 30 μL. For the separation of active ingredients, the mixture of methanol: water (+0.1% H_3PO_4, 50:50 *v/v*) was used as the mobile phase. The mobile phases were passed through a 3.5 μm thick membrane filter, and the flow rate was adjusted to 0.7 mL/min. The active substance concentration was determined by measuring the absorbance at 270 nm [37,38].

2.3. Apparatus

A Nicolet Magna 860 FT-IR spectrometer with a Nicolet Raman unit (Thermo Nicolet, Madison, WI, USA) was used to register the spectra. DRIFTS reflection spectra were obtained using DTGS detector and a Seagull (Harrick, New York, NY, USA) optical assembly set to DRIFTS mode. A KBr beamsplitter was applied to measure the mid-infrared spectra, and a CaF_2 beamsplitter in the NIR region was used. A total of 128 interferograms for NIR measurements and 256 for MIR and Raman were averaged. Interferograms were Happ–Genzel apodized and Fourier transformed using a zero filling factor of 2, giving spectra in the ranges of 400–4000 cm^{-1} for MIR, 3700–10,000 cm^{-1} for NIR and 100–3700 cm^{-1} for Raman with a resolution of 4 cm^{-1}. To register the Raman spectra, an InGaAs detector, CaF_2 beamsplitter, 180° backscattering geometry and a rotating sample holder enabling sample rotation at a constant speed of 200 rpm were applied. The spectra were excited using an Nd: YVO_4 laser with a power of about 400 mW at the sample. All measurements were performed at room temperature.

For the DRIFTS measurements, samples were diluted with potassium bromide, calcined for two hours at 200 °C, at a ratio of 1:49. Pellets for the Raman spectra measurement were prepared.

HPLC analyses were performed using Waters HPLC 600 Quat Pump, 717 Plus Autosampler and 2996 Detector chromatograph (Markham, ON, Canada).

2.4. Software and Numerical Data Treatment

The principal components analysis (PCA) of the obtained data was performed using the PLS Toolbox (ver. 6.2, Eigenvector Research, Wenatchee, WA, USA) in a Matlab R2010a environment (MathWorks, Natwick, MA, USA). TQ Analyst (ver.7, Nicolet, Madison, WI, USA) chemometrics software was used to construct the partial least squares (PLS) models [39,40].

In order to characterize and compare the prognostic abilities of the developed calibration models, the relative standard error of prediction (RSEP) was calculated for the calibration and validation samples, according to the equation:

$$\text{RSEP}(\%) = \sqrt{\frac{\sum_{i=1}^{n} \left(C_i - C_i^A\right)^2}{\sum_{i=1}^{n} C_i^{A^2}}} \times 100, \tag{1}$$

where C_i^A is the actual content of the active substance in the preparation, C_i is content determined on the basis of the model, and *n* is the number of samples [26].

Density functional theory (DFT) calculations were performed at the B3LYP/6-311++G(d,p) level of theory using the Gaussian09 suite of programs [41]. We found all stationary points to be true minima because no imaginary frequencies were obtained.

3. Results and Discussion

3.1. Vibrational Spectra

Raman spectra recorded for the hydrated and anhydrous forms of this flavonoid (Figure S2 in Supplementary Materials) do not show significant changes in the position, shape and intensity of the main vibrational bands. More pronounced differences are observed in the IR spectra (Figure S2 in Supplementary Materials), mainly in the 865–1085, 1350–1670 and 2800–3700 cm^{-1} wavenumber ranges, corresponding to ν(C-O), ν(C-OH) stretching, δ(C-OH), δ(CC-H) deformation and ν(O-H) stretching vibrations [42,43].

These changes result from the presence of a water molecule in the structure of the crystalline form of hydrated diosmin [44]. The most intense bands located in the Raman spectrum at 1501, 1572 and 1611 cm^{-1} and at 1514, 1567 and 1611 cm^{-1} in the DRIFTS/MIR spectrum are attributed to the ν(C=C) stretching of the phenolic ring and δ(C-OH) and δ(CC-H) deformation vibrations. Vibrations of the carbonyl group ν(C=O) result in a band with a maximum at 1660 cm^{-1}. Bands with a maximum at 1142 and 1289 cm^{-1} in the Raman spectrum and at 1142 cm^{-1} in the MIR spectrum are related to the vibrational movements of the C-O-C and C-OH fragments present in diosmin molecules. Stretching vibrations of hydroxyl groups ν(O-H) give bands located in the 3200–3700 cm^{-1} range. Spectral features related to vibrations of the C-OH fragments are observed at 1010, 1074 and 1098 cm^{-1} in the MIR spectrum. Bands at 1453 and 1470 cm^{-1} are assigned to δ(CH$_3$) vibrations of the methyl groups and those located in the 2850–3080 cm^{-1} range in Raman and MIR spectra to ν(C-H) stretching vibrations [42,43]. The assignment of the most important diosmin vibrational bands is summarized in Table S4 in the Supplementary Materials.

The theoretical and experimental IR and Raman spectra of the hydrated (DSNM) and anhydrous (DSNA) forms of diosmin (Figure 2 and Figure S3 in the Supplementary Materials) are very similar, regarding the number and position of the bands, except for the ν(O-H) stretching vibration region. In the theoretical DSNM Raman spectrum, a weak band, located at 1079 cm^{-1}, is shifted toward lower wavenumbers relative to the corresponding DSNA band. This band reflects movements of the C-OH fragments of the compound (Table S4 in the Supplementary Materials). Some changes in the relative intensity of bands are observed, mainly in the 1060–1150, 1530–1670 and 2840–2970 cm^{-1} wavenumber regions. A similar difference is observed in the theoretical IR spectra of the hydrated and anhydrous forms of diosmin (Figure S3 in the Supplementary Materials). In the DSNM spectra, an additional band of medium intensity, with a maximum at 1594 cm^{-1} appears, not observed in the spectrum of its anhydrous form. This band is attributed to deformation vibrations of the hydroxyl group δ(H-OH) of the water molecule present in DSNM. Bands of the symmetrical and asymmetrical stretching vibrations of the water molecule with a maximum at 3507, 3587 and 3812 cm^{-1} are present. The band located in the 1015–1045 cm^{-1} range in the DSNA spectrum consists of two bands, while in the DSNM spectrum, a single, symmetrical band is observed. The most pronounced differences in the relative intensities of the bands are observed in the 965–1120, 1360–1430, 1585–1610 and 2800–3700 cm^{-1} ranges.
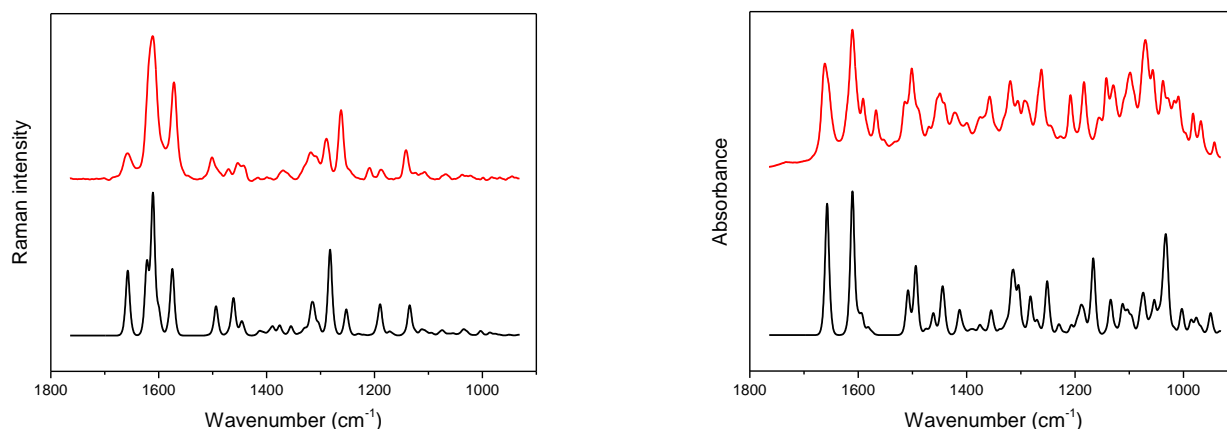
Figure 2. Experimental (red) and calculated (black) Raman (**left**) and IR (**right**) spectra of hydrated diosmin (DSNM); for calculated spectra abscissa scale multiplied by a factor of 0.98; Gauss-Lorentz profile with a half-width of 8.9 cm^{-1} was used to obtain calculated spectra.

Despite the superficial similarity of IR spectra of both diosmin forms (Figure S2 in the Supplementary Materials), the contribution of the water molecule present in the crystal structure of DSNM is clearly visible in the difference spectrum. A broad band located approximately at 3300 cm^{-1} can be assigned to the ν(O–H) stretching vibrations of the hydrogen-bonded water molecule. Additionally, in the difference spectrum, the contribution resulting from changes in a δ(CC–H) deformation and ν(C=C) stretching vibrations of the hydrated and anhydrous form carbohydrate fragment can be noticed in the 1375–1550 cm^{-1} wavenumber range. In the IR difference spectrum obtained from the DFT calculation, bands with maxima at 1594, 3507, 3587 and 3812 cm^{-1} are observed.

The recorded NIR spectra of the hydrated and anhydrous forms of diosmin (Figure S2 in Supplementary Materials) show no pronounced differences, except in the 4400–5200 and 6200–7000 cm^{-1} ranges. A broad band of medium intensity, with a maximum at 6737 cm^{-1}, can be attributed to the first overtone of the hydroxyl group stretching vibrations and those located at around 6000 cm^{-1} to the first overtones of the ν(C–H) vibrations. In the 4800–4890 cm^{-1} frequency range, combination bands of ν(O–H) and ν(C=C) stretching vibrations are present [44–47]. In the NIR difference spectrum of the hydrated and anhydrous forms of diosmin, bands that can be attributed to the vibrations of the water molecule bonded to the diosmin carbohydrate fragment are observed at 4490 and 6950 cm^{-1} [48].

FT-Raman, DRIFTS/MIR and DRIFTS/NIR spectra of the representative calibration sample and the studied pharmaceutical preparations are shown in Figure 3. The analyzed preparations, apart from API, the content of which varied in the 65.3–89.4% range as declared by the manufacturers, contained croscarmellose sodium, carboxymethyl starch, microcrystalline cellulose or starch, polyvinyl alcohol or povidone and magnesium stearate or stearic acid. In some of them, colloidal silica and talk were also present. Detailed data on the composition of the analyzed preparations is presented in Table S1 in Supplementary Materials. Despite the slightly different chemical compositions of the analyzed tablets, their vibrational spectra are similar to each other. These differences become visible in the space of the first two principal components (PC1/PC2) (Figure 3). Figure S4 in Supplementary Materials shows the loadings plots for PC1 and PC1 principal components obtained on the basis of Raman, MIR and NIR spectra of calibration samples.
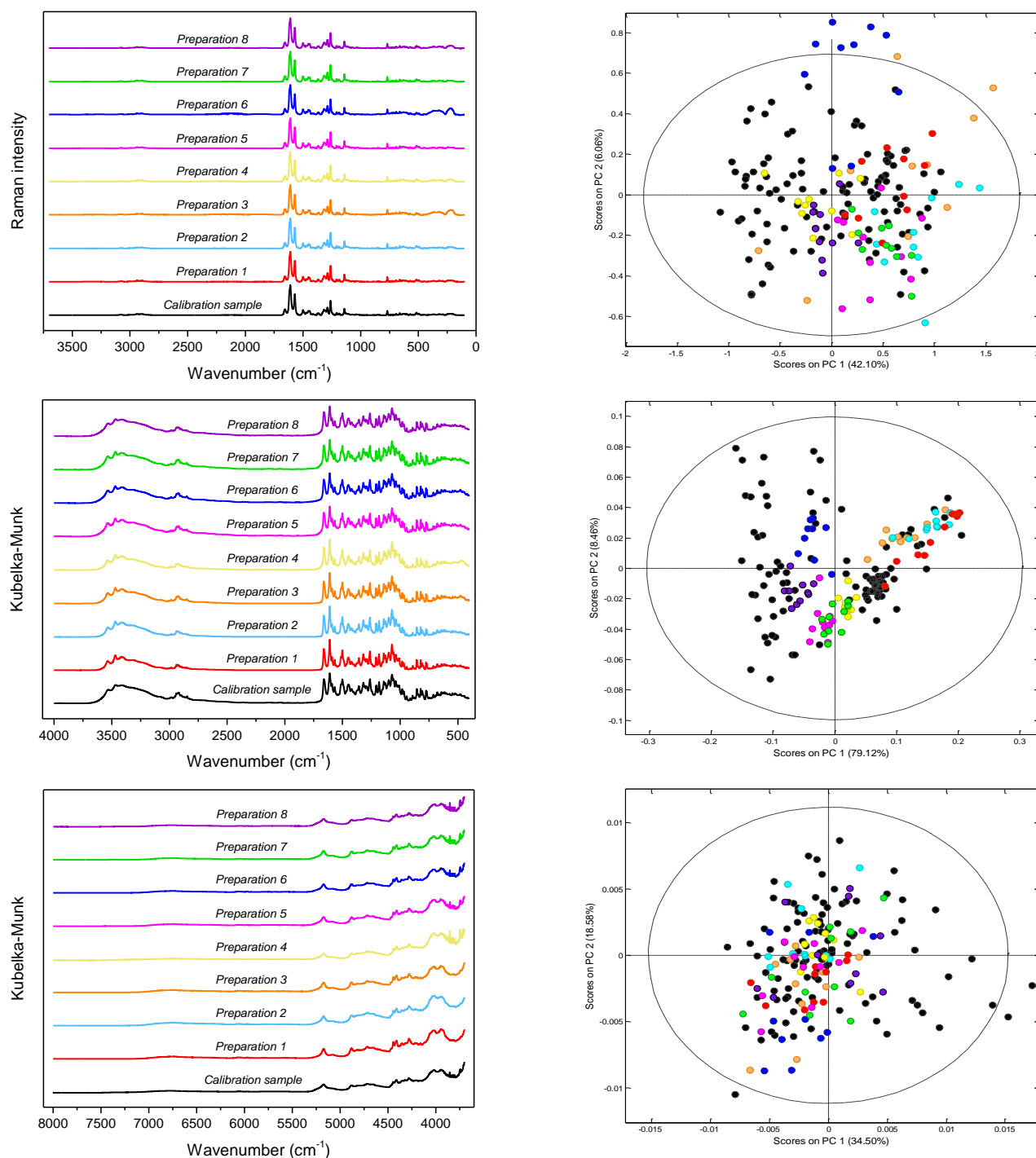
Figure 3. From the top: Raman, MIR and NIR spectra (**left**) of the studied preparations and distribution of samples in the PC1/PC2 space with the 99% confidence interval (**right**); black dots—calibration mixtures, colored dots—pharmaceutical tablets.

3.2. Chemometric Analysis

Keeping in mind that diosmin contributes from approximately 65 to 90% of the analyzed preparations and the fact that the excipients present are the same or related chemical compounds, we have decided to prepare calibration samples composed of diosmin, polyvinyl alcohol, sodium croscarmellose and magnesium stearate. Their mass fractions ranged from 0.603 to 0.926 for diosmin, from 0.005 to 0.054 for magnesium stearate, from 0.016 to 0.222 for polyvinyl alcohol and from 0.017 to 0.202 for sodium croscarmellose. In

the prepared mixtures, concentrations of individual components did not correlate with each other. A set of 83 samples was used to construct PLS models, with approximately 25% of them selected using a bootstrap method and a sample distribution in PC1/PC2 space as test samples. Some of them have been omitted, but not more than 10 in each case. We summarize the type of spectra preprocessing and spectral ranges selected for analysis in Table 1 and Table S5 in Supplementary Materials. Figure S5 in Supplementary Materials shows regression vectors obtained on the basis of Raman, MIR and NIR spectra of calibration samples.

**Table 1.** Parameters of PLS models developed for Preparation 1.

Parameter	RAMAN	MIR	NIR
R_{cal}	0.9920	0.9882	0.9905
R_{test}	0.9932	0.9838	0.9877
R_{cv}	0.9641	0.9536	0.9568
$RSEP_{cal}$	1.30	1.41	1.32
$RSEP_{test}$	1.25	1.59	1.39
Number of PLS factors	5	7	7
Wavenumber range [cm^{-1}]	488–963	1478–1633	3811–3957
	3036–3119	2391–3452	4379–4762
			6153–6683
Normalization	SNV	None	SNV

R—correlation coefficient, R_{CV}—correlation coefficient of cross-validation, cal—calibration set, test—test set, SNV—standard normal variate.

To assess the spectral identity of the prepared calibration mixtures and the commercial diosmin preparations, PCA was performed. For each of the applied spectroscopic techniques, points corresponding to the analyzed preparations, as shown in Figure 3, are evenly distributed in the PC1/PC2 space, constructed based on calibration sample spectra. To determine diosmin content, PLS models were developed for each of the analyzed preparations and techniques applied separately. Spectral ranges selected for the analysis differ slightly depending on the preparation, due to the differences in the composition of tablets originating from different manufacturers, as we have mentioned before. Elaborated PLS models are of similar quality within a given spectroscopic technique. Relative standard errors of prediction are in the range of 1.0–2.4% and 1.1–2.4% for the calibration and test sample sets, respectively (Table 1 and Table S5 in Supplementary Materials). Internal validation of the models using a leave-one-out (LOO) procedure resulted in correlation coefficients of cross-validation in the 0.944–0.964 range. Characteristics of the constructed models are presented in Figure 4, Table 1 and Table S5 in Supplementary Materials. The number of latent variables (5, 6 or 7) was selected based on the RMSECV plots. We determined the diosmin content on the basis of vibrational spectra of the analyzed tablets with a recovery of 99.5–100.5% (Figure 5) with a standard deviation varying in the 0.6–3.4% range (Table S6 in Supplementary Materials). Selectivity ratio (SR), presented in Figure 4, shows spectral contributions of the variables in the projection used in the PLS models. For Raman data, the highest contributions are observed in the frequency range of 1000–1750 cm^{-1} and 490–790 cm^{-1}. For MIR data, regions 1000–1800 cm^{-1} and 3000–3700 cm^{-1} are the most important, while for NIR data, these contributions are large in the 4050–5300 and 6900–7250 cm^{-1} ranges.
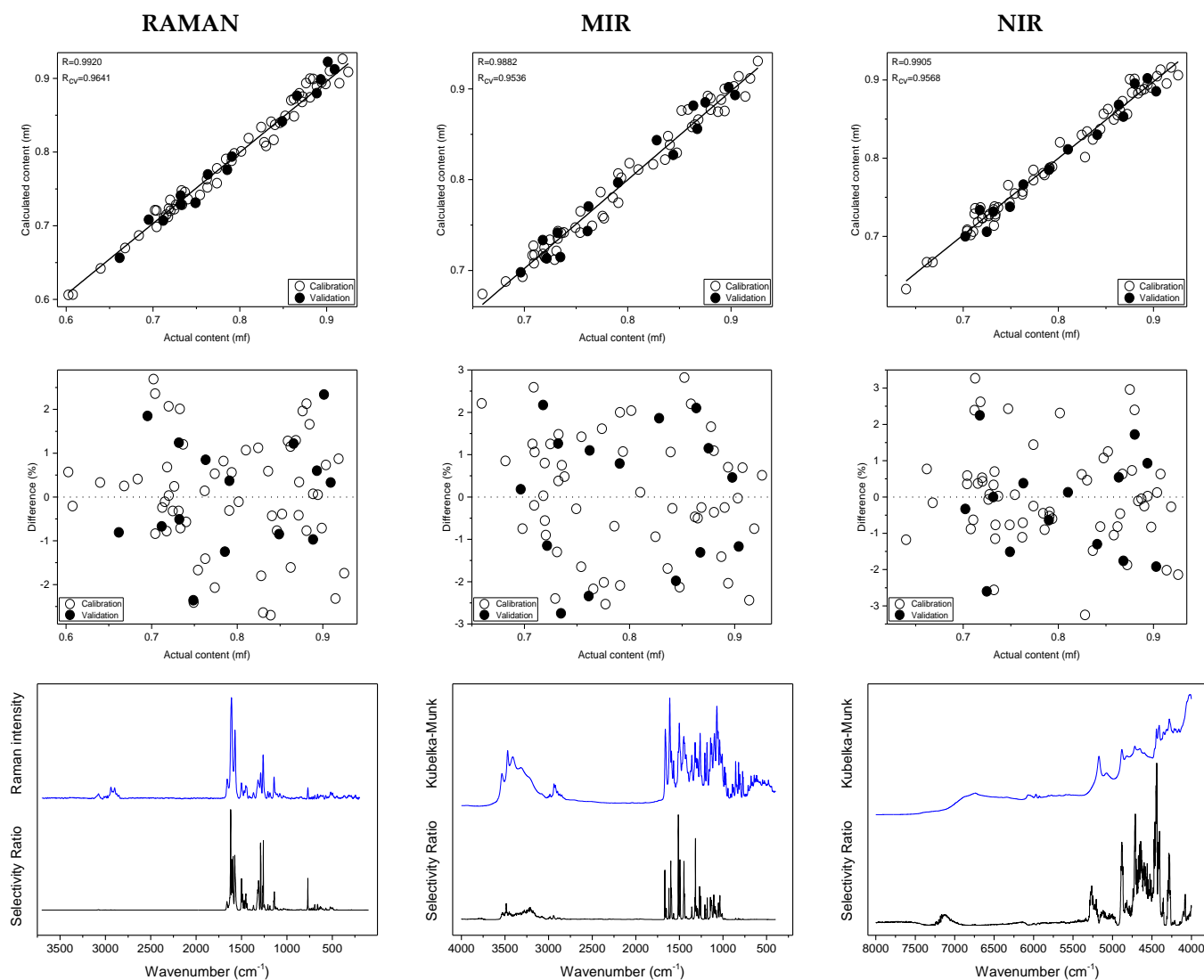
Figure 4. Prediction plots, relative errors, experimental spectra of hydrated diosmin (DSNM) (blue) and selectivity ratio (SR) (black) obtained on the basis of Raman, MIR and NIR spectra of calibration samples for Preparation 1; from the top.
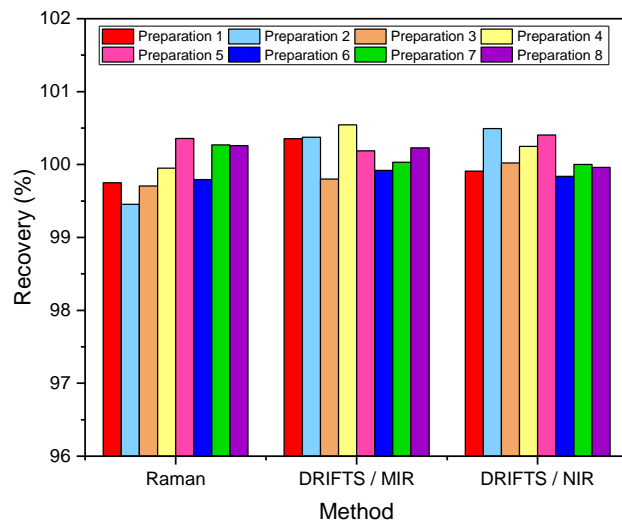
Figure 5. Diosmin recovery (*n* = 10).

A similar analysis was performed based on ATR data for selected diosmin preparations, and results of comparable quality were obtained.

4. Conclusions

Here, for the first time, the suitability of Raman and NIR spectroscopy for the determination of diosmin content in intact pharmaceutical preparations was demonstrated. Eight commercial tablets containing diosmin as an active ingredient in the 66–92% (*w/w*) range were successfully quantified using PLS models based on Raman and infrared reflection spectra of powdered tablets in the mid- and near-infrared regions, with an error below 2.4%. The concentration of diosmin in commercial pharmaceutical preparations determined based on PLS models is consistent with the results of the reference analysis with a recovery of 99.5–100.5%. The quality of determinations is comparable for the three methods used. The described procedure enables efficient, fast and reliable quantification of active ingredients in tablets, supporting the analysis of pharmaceutical products containing diosmin.

Supplementary Materials: The following supporting information can be downloaded at: https://www.mdpi.com/article/10.3390/molecules27238276/s1, Figure S1: Raman, MIR and NIR spectra of Preparation 1, diosmin hydrate, polyvinyl alcohol, croscarmellose sodium and magnesium stearate, Figure S2: Experimental Raman, MIR and NIR spectra of hydrated (DSNM) and anhydrous (DSNA) diosmin, Figure S3: Calculated Raman and IR spectra of hydrated (DSNM) and anhydrous (DSNA) diosmin, Figure S4: Loadings plots of PCA models obtained on the basis of Raman, MIR and NIR spectra of calibration samples, Figure S5: Regression vectors obtained on the basis of Raman, MIR and NIR spectra of calibration samples, Table S1: Basic data on the analyzed preparations, Table S2: Composition of calibration samples, Table S3: API content in the studied preparations, Table S4: Band assignment in the Raman and MIR spectra of diosmin, Table S5: Parameters of PLS models for preparations 2–8, Table S6: Diosmin recovery.

Author Contributions: Conceptualization, R.S.; methodology, R.S.; investigation, M.W., S.P., R.S.; data curation, M.W., S.P., S.M.; analysis and validation, S.P., M.W., S.M., R.S.; writing—original draft preparation, S.P.; writing—review and editing, R.S., S.P., S.M.; supervision, R.S. All authors have read and agreed to the published version of the manuscript.

References

1. El-Shafae, A.M.; El-Domiaty, M.M. Improved LC methods for the determination of diosmin and/or hesperidin in plant extracts and pharmaceutical formulations. *J. Pharm. Biomed. Anal.* **2001**, *26*, 539–545. [CrossRef]
2. Diosmin Monograph. *Altern. Med. Rev.* **2004**, *9*, 308–311.
3. Bogucka–Kocka, A.; Woźniak, M.; Feldo, M.; Kocki, J.; Szewczyk, K. Diosmin–isolation techniques, determination in plant material and pharmaceutical formulations, and clinical use. *Nat. Prod. Commun.* **2013**, *8*, 545–550. [CrossRef]
4. Garner, R.C.; Garner, J.V.; Gregory, S.; Whattam, M.; Calam, A.; Leong, D. Comparison of the absorption of micronized (Daflon 500® mg) and nonmicronized ¹⁴C-diosmin tablets after oral administration to healthy volunteers by accelerator mass spectrometry and liquid scintillation counting. *J. Pharm. Sci.* **2002**, *91*, 32–40. [CrossRef]
5. López Cremades, F.J. Process for the preparation of diosmin. U.S. Patent US 10,711,025 B2, 14 July 2020.
6. Nguyen, V.T.; Huynh, T.; Nguyen, T.D.; Hoang, T. Oxidation of hesperidin into diosmin using ionic liquids. *Org. Commun.* **2019**, *12*, 101–108. [CrossRef]
7. Horowitz, R. Flavonoids of citrus. I. Isolation of diosmin from lemons (Citrus limon). *J. Org. Chem.* **1956**, *21*, 1184–1185. [CrossRef]

8. Del Río, J.A.; Fuster, M.D.; Gómez, P.; Porras, I.; García-Lidón, A.; Ortuño, A. Citrus limon: A source of flavonoids of pharmaceutical interest. *Food Chem.* **2004**, *84*, 457–461. [CrossRef]

9. Hitzenberger, G. Therapeutic effectiveness of flavonoids illustrated by Daflon 500 mg. *Wien. Med. Wochenschr. 1997 147*, 409–412.

10. Ibegbuna, V.; Nicolaides, A.N.; Sowade, O.; Leon, M.; Geroulakos, G. Venous elasticity after treatment with Daflon 500 mg. *Angiology* **1997**, *48*, 45–49. [CrossRef]

11. Cospite, M.; Dominici, A. Double blind study of the pharmacodynamic and clinical activities of 5682 SE in venous insufficiency. Advantages of the new micronized form. *Int. J. Angiol.* **1989**, *8*, 61–65.

12. Takase, S.; Lerond, L.; Bergan, J.J.; Schmid-Schönbein, G.W. The inflammatory reaction during venous hypertension in the rat. *Microcirculation* **2000**, *7*, 41–52. [CrossRef] [PubMed]

13. Galley, P.; Thiollet, M. A double-blind, placebo-controlled trial of a new veno-active flavonoid fraction (S 5682) in the treatment of symptomatic capillary fragility. *Int. J. Angiol.* **1993**, *12*, 69–72.

14. Shoab, S.S.; Porter, J.B.; Scurr, J.H.; Coleridge-Smith, P.D. Effect of oral micronized purified flavonoid fraction treatment on leukocyte adhesion molecule expression in patients with chronic venous disease: A pilot study. *J. Vasc. Surg.* **2000**, *31*, 456–461. [CrossRef] [PubMed]

15. Allegra, C.; Bartolo, M.; Carioti, B.; Cassiani, D.; BesseBoffi, M.G. Microlymphography: Assessment of Daflon 500 mg activity in patients with chronic venous insufficiency. *Lymphology* **1998**, *31*, 12–16.

16. Ratty, A.K.; Das, N.P. Effects of flavonoids on nonenzymatic lipid peroxidation: Structure-activity relationship. *Biochem. Med. Metab. Biol.* **1988**, *39*, 69–79. [CrossRef] [PubMed]

17. Tanaka, T.; Kohno, H.; Mori, H. Chemoprevention of colon carcinogenesis by dietary non-nutritive compounds. *Asian Pac. J. Cancer Prev.* **2001**, *2*, 165–177.

18. Srinivasan, S.; Pari, L. Ameliorative effect of diosmin, a citrus flavonoid against streptozotocin-nicotinamide generated oxidative stress induced diabetic rats. *Chem. Biol. Interact.* **2012**, *195*, 43–51. [CrossRef]

19. Janeczko, Z.; Hubicka, U.; Krzek, J.; Podolak, I. Qualitative and quantitative analysis of diosmin in tablets by thin layer chromatography with densitometric UV detection. *JPC-J. Planar Chromat.* **2003**, *16*, 377–380. [CrossRef]

20. El-Shahawi, M.S.; Bashammakh, A.S.; El-Mogy, T. Determination of trace levels of diosmin in a pharmaceutical preparation by adsorptive stripping voltammetry at a glassy carbon electrode. *Anal. Sci.* **2006**, *22*, 1351–1354. [CrossRef]

21. Gunache, R.O.; Apetrei, C. Determination of diosmin in pharmaceutical products with chemically modified voltammetric Sensors. *Int. J. Mol. Sci.* **2021**, *22*, 7315. [CrossRef]

22. Moldovan, Z.; Aboul-Enein, H.Y. A sensitive spectrophotometric method for determination of diosmin using sodium nitroprusside as a chromogenic reagent. *Instrum. Sci. Technol.* **2011**, *39*, 135–148. [CrossRef]

23. Moldovan, Z.; Bunaciu, A.A.; Al-Omar, M.A.; Aboul-Enein, H.Y. A spectrophotometric method for diosmin determination. *Open Chem. Biomed. Meth. J.* **2010**, *3*, 123–127.

24. Bunaciu, A.A.; Udristioiu, G.E.; Ruţă, L.L.; Fleschin, Ş.; Aboul-Enein, H.Y. Determination of diosmin in pharmaceutical formulations using Fourier transform infrared spectrophotometry. *Saudi Pharm. J.* **2009**, *17*, 303–306. [CrossRef]

25. Mazurek, S.; Szostak, R. Comparison of infrared attenuated total reflection and Raman spectroscopy in the quantitative analysis of diclofenac sodium in tablets. *Vib. Spectrosc.* **2011**, *57*, 157–162. [CrossRef]

26. Szostak, R.; Mazurek, S. Quantitative determination of acetylsalicylic acid and acetaminophen in tablets by FT-Raman spectroscopy. *Analyst* **2002**, *127*, 144–148. [CrossRef]

27. Roggo, Y.; Chalus, P.; Maurer, L.; Lema-Martinez, C.; Edmond, A.; Jent, N. A review of near infrared spectroscopy and chemometrics in pharmaceutical technologies. *J. Pharm. Biomed. Anal.* **2007**, *44*, 683–700. [CrossRef]

28. Grassi, S.; Alamprese, C. Advances in NIR spectroscopy applied to process analytical technology in food industries. *Curr. Opin. Food Sci.* **2018**, *22*, 17–21. [CrossRef]

29. Mauer, L.J.; Chernyshova, A.A.; Hiatt, A.; Derring, A.; Davis, R. Melamine detection in infant formula powder using near- and mid-infrared spectroscopy. *J. Agric. Food Chem.* **2009**, *57*, 3974–3980. [CrossRef]

30. Patel, B.D.; Mehta, P.J. An overview: Application of Raman spectroscopy in pharmaceutical field. *Curr. Pharm. Anal.* **2010**, *6*, 131–141. [CrossRef]

31. Townshend, N.; Nordon, A.; Littlejohn, D.; Myrick, M.; Andrews, J.; Dallin, P. Comparison of the determination of a low-concentration active ingredient in pharmaceutical tablets by backscatter and transmission Raman spectrometry. *Anal. Chem.* **2012**, *84*, 4671–4676. [CrossRef]

32. Bonnier, F.; Petitjean, F.; Baker, M.J.; Byrne, H.J. Improved protocols for vibrational spectroscopic analysis of body fluids. *J. Biophoton.* **2014**, *7*, 167–179. [CrossRef] [PubMed]

33. Kendall, C.; Isabelle, M.; Bazant-Hegemark, F.; Hutchings, J.; Orr, L.; Babrah, J.; Stone, N. Vibrational spectroscopy: A clinical tool for cancer diagnostics. *Analyst* **2009**, *134*, 1029–1045. [CrossRef] [PubMed]

34. Bell, S.E. Quantitative Analysis of Solid Dosage Formulations by Raman Spectroscopy. In *Pharmaceutical Applications of Raman Spectroscopy*; Šašić, S., Ed.; John Wiley & Sons: Hoboken, NJ, USA, 2007; pp. 29–64.

35. Gredilla, A.; Fdez-Ortiz de Vallejuelo, S.; Elejoste, N.; de Diego, A.; Madariaga, J.M. Non-destructive spectroscopy combined with chemometrics as a tool for green chemical analysis of environmental samples: A review. *TrAC* **2016**, *76*, 30–39. [CrossRef]

36. Szeleszczuk, Ł.; Pisklak, D.M.; Zielińska-Pisklak, M.; Wawer, I. Spectroscopic and structural studies of the diosmin monohydrate and anhydrous diosmin. *Int. J. Pharm.* **2017**, *529*, 193–199. [CrossRef]

37. Saeidi, I.; Hadjmohammadi, M.R.; Peyrovi, M.; Iranshahi, M.; Barfi, B.; Babaei, A.B.; Dust, A.M. HPLC determination of hesperidin, diosmin and eriocitrin in Iranian lime juice using polyamide as an adsorbent for solid phase extraction. *J. Pharm. Biomed. Anal.* **2011**, *56*, 419–422. [CrossRef]

38. Mishra, G.; Srivastava, V.K.; Tripathi, A. Analytical method development and validation for assay of diosmin and hesperidin in combined tablet dosage form by RP-HPLC. *Int. J. Pharm. Biol. Sci.* **2013**, *4*, 2834–2839.

39. Geladi, P.; Kowalski, B.R. Partial least-squares regression: A tutorial. *Anal. Chim. Acta* **1986**, *185*, 1–17. [CrossRef]

40. Wise, B.M.; Kowalski, B.R. Process chemometrics. In *Process Analytical Chemistry*; McLennan, F., Kowalski, B.R., Eds.; Springer: Dordrecht, The Netherlands, 1995; pp. 259–312.

41. Frisch, M.J.; Trucks, G.W.; Schlegel, H.B.; Scuseria, G.E.; Robb, M.A.; Cheeseman, J.R.; Scalmani, G.; Barone, V.; Petersson, G.A.; Nakatsuji, H.; et al. *Gaussian 09, Revision A.02*; Gaussian, Inc.: Wallingford, CT, USA, 2016.

42. Naso, L.; Martínez, V.R.; Lezama, L.; Salado, C.; Valcarcel, M.; Ferrer, E.G.; Williams, P.A. Antioxidant, anticancer activities and mechanistic studies of the flavone glycoside diosmin and its oxidovanadium (IV) complex. Interactions with bovine serum albumin. *Bioorg. Med. Chem.* **2016**, *24*, 4108–4119. [CrossRef]

43. Aghel, N.; Ramezani, Z.; Beiranvand, S. Hesperidin from Citrus sinensis cultivated in Dezful, Iran. *Pak. J. Biol. Sci.* **2008**, *11*, 2451–2453. [CrossRef]

44. Jurczak, E.; Mazurek, A.H.; Szeleszczuk, Ł.; Pisklak, D.M.; Zielińska-Pisklak, M. Pharmaceutical Hydrates Analysis-Overview of Methods and Recent Advances. *Pharmaceutics* **2020**, *12*, 959. [CrossRef]

45. Mazurek, S.; Włodarczyk, M.; Pielorz, S.; Okińczyc, P.; Kuś, P.M.; Długosz, G.; Szostak, R. Quantification of salicylates and flavonoids in poplar bark and leaves based on IR, NIR, and Raman spectra. *Molecules* **2022**, *27*, 3954. [CrossRef] [PubMed]

46. Guo, Z.; Barimah, A.O.; Yin, L.; Chen, Q.; Shi, J.; El-Seedi, H.R.; Zou, X. Intelligent evaluation of taste constituents and polyphenols-to-amino acids ratio in matcha tea powder using near infrared spectroscopy. *Food Chem.* **2021**, *353*, 129372. [CrossRef]

47. Stuppner, S.; Mayr, S.; Beganovic, A.; Beć, K.; Grabska, J.; Aufschnaiter, U.; Groeneveld, M.; Rainer, M.; Jakschitz, T.; Bonn, G.K.; et al. Near-infrared spectroscopy as a rapid screening method for the determination of total anthocyanin content in Sambucus fructus. *Sensors* **2020**, *20*, 4983. [CrossRef] [PubMed]

48. Gowen, A.A.; Marini, F.; Tsuchisaka, Y.; De Luca, S.; Bevilacqua, M.; O'Donnell, C.; Downey, G.; Tsenkova, R. On the feasibility of near infrared spectroscopy to detect contaminants in water using single salt solutions as model systems. *Talanta* **2015**, *131*, 609–618. [CrossRef] [PubMed]